Tail current surge: New insights from a global MHD simulation and comparison with satellite observations

Shin-ichi Ohtani

Applied Physics Laboratory, Johns Hopkins University, Laurel, Maryland, USA

Joachim Raeder[1]

Institute of Geophysics and Planetary Physics, University of California, Los Angeles, Los Angeles, California, USA

Received 25 October 2002; revised 19 August 2003; accepted 2 October 2003; published 14 January 2004.

[1] The present study examines the tailward propagation of substorm-associated variations of the tail current intensity. In the substorm event of 24 November 1996, the Interball and IMP 8 satellites were located in the midnight sector at $X = -26$ and -36 R_E, respectively, and observed an increase and a decrease of the lobe magnetic field strength corresponding to the storage and release of the lobe magnetic energy. Both spacecraft observed B_Z to decrease initially and then increase in the course of the decrease in $|B_X|$, a feature that was reported previously as a manifestation of the tailward expansion of the current disruption region. The delay of the signatures between the two satellites confirms that the associated current system moved tailward. Motivated by this fortuitous coordination of the satellite observation, the present study revisits a global MHD simulation previously conducted specifically for this substorm event [*Raeder et al.*, 2001]. The most noticeable feature of the modeled tail dynamics is the repeated occurrence of tail current surges, that is, temporal intensifications of the tail current that propagate tailward. The first tail current surge is accompanied by the stretching of the tail magnetic field, which starts in the inner magnetosphere and extends tailward. The associated tailward flow redistributes the plasma pressure in such a way that the tail current is reduced in its intensity in the near-Earth region, while the pressure gradient increases at the propagation front, which intensifies the local current. The last major tail current surge is caused by the near-Earth reconnection. Inside a plasmoid, the pressure gradient current is intensified on the tailward side of the *O*-line, and it propagates tailward as the plasmoid grows and is released. For each tail current surge, irrespective of its cause, the intensification of the tail current is followed by the reduction, and its tailward propagation creates the aforementioned phase relationship between B_X and B_Z. It is probably difficult to determine based on lobe magnetic field observations whether it is caused by the tail stretching or a neutral line motion. The present study not only sheds new light about tail substorm dynamics but also provides a good exercise for evaluating the potential of the modeling effort for substorm study in general. *INDEX TERMS:* 2788 Magnetospheric Physics: Storms and substorms; 2708 Magnetospheric Physics: Current systems (2409); 2744 Magnetospheric Physics: Magnetotail; 2740 Magnetospheric Physics: Magnetospheric configuration and dynamics; 2753 Magnetospheric Physics: Numerical modeling; *KEYWORDS:* substorm, magnetotail, tail current, growth phase, near-Earth reconnection, global MHD simulation

Citation: Ohtani, S., and J. Raeder (2004), Tail current surge: New insights from a global MHD simulation and comparison with satellite observations, *J. Geophys. Res.*, *109*, A01207, doi:10.1029/2002JA009750.

1. Introduction

[2] The poleward auroral expansion following the expansion onset is one of the most fundamental features of the auroral substorm [*Akasofu*, 1964]. The auroral expansion starts well equatorward of the open-close boundary and then progresses poleward [*Samson et al.*, 1992; *Friedrich et al.*, 2001]. Such auroral development presumably corresponds to the tailward expansion or propagation of an active region in the near-Earth plasma sheet.

[3] The substorm-associated tail electrodynamics has been considered in terms of a three-dimensional (3-D) current system called substorm wedge current. This model is based on the idea that during substorms, the tail current intensity is locally reduced, which is inferred from the

[1]Now at Space Science Center, University of New Hampshire, Durham, New Hampshire, USA.

Copyright 2004 by the American Geophysical Union.
0148-0227/04/2002JA009750$09.00

change of the tail magnetic field from a stretched to a dipolar configuration [e.g., *Cummings et al.*, 1968]. In the newly formed current circuit, the tail current is partly closed with field-aligned currents flowing toward and away from the ionosphere on the morning and evening sides, respectively, which are closed by an enhanced westward electrojet in the ionosphere [*McPherron et al.*, 1973]. It is inferred from the auroral morphology that during the expansion phase, the source region, or the current disruption region, expands tailward [*Akasofu*, 1972].

[4] Multisatellite observations have revealed that the dipolarization region indeed expands tailward [*Ohtani et al.*, 1988; *Lopez and Lui*, 1990]. It was also found that B_X and B_Z in the tail lobe occasionally change in a coherent way that can be interpreted in terms of the tailward expansion of the current disruption region [*Jacquey et al.*, 1991, 1993; *Ohtani et al.*, 1992], though this feature can be explained alternatively in terms of the tailward motion of a neutral line.

[5] Although the aforementioned fact may give an impression that the magnetospheric substorm is triggered by tail current disruption in the near-Earth region, the issue of the substorm trigger is far more complex. Whereas the tail current disruption model [e.g., *Lui*, 1996] describes the substorm from the viewpoint of electric current, the magnetic reconnection model, or the near-Earth neutral line model [e.g., *Baker et al.*, 1996], addresses the transport of the magnetic flux from the nightside to dayside. Causal relationship between tail current disruption and near-Earth reconnection has been controversial for a long time.

[6] The currently most popular model, which is called the pile-up model or the braking model, is based on the idea that first the NENL is formed in the midtail region. The model describes near-Earth dipolarization as the pile-up of the magnetic flux transported from the NENL [e.g., *Hesse and Birn*, 1991], and it explains tail current disruption in terms of the inertia current induced by the flow braking [*Shiokawa et al.*, 1998] or the pressure gradient current driven by the associated changes of the plasma and magnetic field distributions [*Birn et al.*, 1999]. The model is supported (but not proved) by the occasional detection of fast plasma flows before substorm/Pi2 onsets [e.g., *Nagai et al.*, 1998; *Shiokawa et al.*, 1998] and by a fortuitous event in which various substorm identifiers, including the ejection of a plasmoid several minutes before an expansion onset, were observed in the predicted order [e.g., *Ohtani et al.*, 1999].

[7] An alternative model of the substorm trigger process proposes that tail current disruption launches a rarefaction wave, which sets up a favorable condition for a NENL to form farther tailward [*Chao et al.*, 1977; *Lui*, 1991; *Erickson et al.*, 2000]. The list of candidate mechanisms for the near-Earth trigger includes the cross-field current instability [*Lui et al.*, 1991], which was recently generalized to encompass the lower hybrid drift instability, the drift sausage/kink instability [*Yoon et al.*, 1998; *Yoon and Lui*, 2001], and the ballooning instability [*Roux et al.*, 1991; *Cheng and Lui*, 1998].

[8] Both the pile-up/braking and rarefaction wave models have a difficulty in explaining the aforementioned lobe magnetic signature that have been regarded as a manifestation of the tailward expansion of the current disruption region. As will be shown in section 2, B_Z in the tail lobe decreases prior to local dipolarization, which is just the opposite to what one would expect from the pile-up of the magnetic flux. On the other hand, the rarefaction wave model has a difficulty in explaining the expansion velocity. Whereas the observed propagation velocity of tail current disruption is 300–400 km/s [*Jacquey et al.*, 1991, 1993; *Ohtani et al.*, 1992], the thermal velocity of 5 keV protons is about 1000 km/s, and therefore the perpendicular propagation velocity of the fast magnetosonic mode, which carries the rarefaction wave, is even faster. Thus the tailward expansion of current disruption cannot be regarded as a direct manifestation of the rarefaction wave. For the better understanding of the spatial development of the tail current disruption, it would be ideal if we could address it in the context of the global substorm dynamics.

[9] In the present study we examine the tailward propagation of a substorm current system in the substorm event of 24 November 1996. This event was examined previously in terms of the force (im)balance between the plasmasheet and the tail lobe [*Petrukovich et al.*, 1999]. Recently the event was selected as a substorm challenge event by the National Science Foundation/Geospace Environment Modeling (NSF/GEM) community and was examined from various viewpoints (see the preface given by *Raeder and Maynard* [2001] and other companion papers in the same issue). An ideally simple IMF condition and excellent satellite coordination in the magnetotail for this event have provided a unique opportunity for evaluating global MHD simulations based on satellite and ground observations. We recently noticed that lobe magnetic field signatures observed by the Interball and IMP 8 satellites in this event are very similar to what has been reported as an indication of the tailward expansion of the current disruption region. This finding motivated us to reexamine a global MHD simulation that was conducted before specifically for this event [*Raeder et al.*, 2001].

[10] In section 2.1 we describe the 24 November 1996 event with an emphasis on magnetic signatures observed by the Interball and IMP 8 satellites in the tail lobe. After summarizing the overall sequence of the modeled tail substorm in section 3.1, we compare in section 3.2 the observations with the simulated lobe magnetic signatures at the satellite positions. In section 3.3 we examine how the radial profile of the tail current intensity and the associated plasma parameters change in the course of the event in the simulated magnetosphere. A focus will be placed on repeated formation of tail current surges. The results are discussed and summarized in section 4.

2. The 24 November 1996 Event

[11] On 24 November 1996 the Wind satellite was in the solar wind at (73, −18, 8) R_E in GSM. The travel time from the satellite to the dayside magnetopause is estimated at 18 min. Wind observed predominantly northward IMF until 2044 UT; then the IMF rapidly turned southward [*Raeder and Maynard*, 2001; *Lyons et al.*, 2001]. The IMF B_Z stayed around −7 nT for more than 90 min and then turned northward again at 2220 UT. The Polar/VIS data reveal the first substorm-related auroral brightening at 2227 UT, which was accompanied by the simultaneous (<1 min) starts

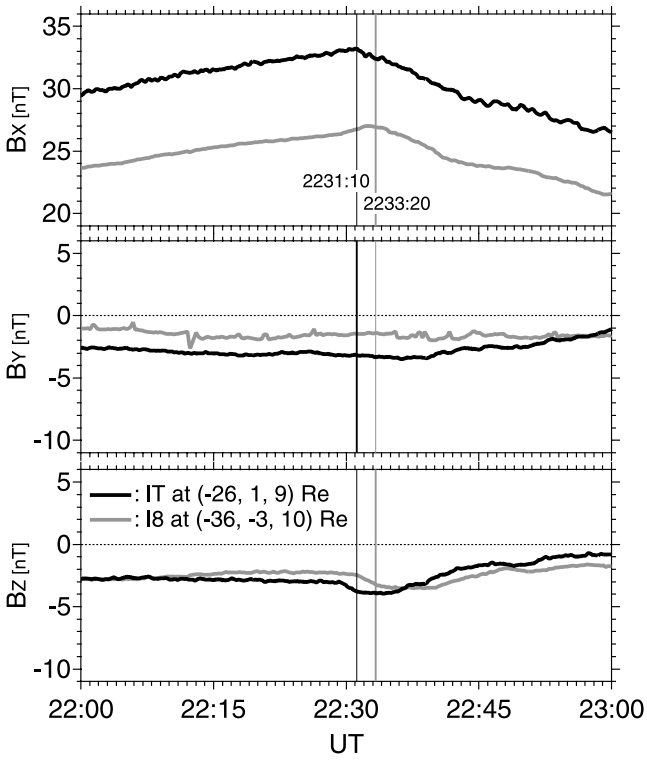

Figure 1. Three magnetic field components in GSM measured by the Interball (black) and IMP 8 (gray) satellites for 2200–2300 UT on 24 November 1996.

of various ground signatures such as a high-latitude negative bay and a Pi2 pulsation [*Lyons et al.*, 2001].

[12] Figure 1 plots the three magnetic field components measured by the Interball (black) and IMP 8 (gray) satellites for 2200–2300 UT. For comparing later with the result of the simulation, the GSE coordinate system, rather than the GSM coordinate system, is used for magnetic field data throughout this paper. However, those systems differ by less than 2° throughout the interval, and therefore they can be practically regarded as the same. The Interball/Tail and IMP-8 satellites were located at (−26.4, 1.3, 9.3) and (−36.2, −2.9, 10.4) R_E in GSM, respectively, in the midnight sector at 2230 UT. The predominantly earthward magnetic field along with its large (>20 nT) magnitude indicates that both satellites were located in the northern tail lobe. Thus the magnetic measurements should not be very sensitive to the spacecraft distance from the neutral sheet, which is favorable for the comparison with the results of the global simulation. The larger magnitude of B_X at Interball than at IMP 8 can be attributed to its location closer to the Earth.

[13] At both satellites, B_X increased monotonically until a little after 2230 UT, which corresponds to the inflation of the lobe magnetic flux owing to the southward IMF B_Z. B_X started to decrease at 2231:10 and 2233:20 UT (marked by the vertical lines in Figure 1a) at Interball and IMP 8, respectively, suggesting the release of the lobe magnetic energy. At Interball, B_Z started to decrease around 2230 UT followed by an equally gradual recovery. IMP 8 observed a similar B_Z signature, which was trailed by the Interball signature as was found for B_X. No characteristic feature can be found for B_Y except for small variations, which seem to be the projection of the variations of the other components.

[14] Here the source current is inferred to be flowing in the Y direction, and it is therefore most likely to be the tail current. The initial increase and following decrease in B_X can be attributed to the intensification and reduction of the tail current, and the time delay between the two spacecraft indicates that these changes propagated tailward. Furthermore, the variation of B_Z and its timing relative to the B_X decrease is very similar to what was reported previously as an indication of the tailward expansion of the current disruption region [*Jacquey et al.*, 1991, 1993; *Ohtani et al.*, 1992].

[15] Figure 2 illustrates the explanation proposed by those studies. Magnetic effects of tail current disruption can be envisioned by superposing a perturbation current flowing in the opposite direction to the tail current, that is, from dusk to dawn, which is represented by current elements flowing into the figure. When current disruption occurs on the earthward (Figure 2a) and tailward (Figure 2c) sides, the resultant magnetic variation is directed southward and northward, respectively. If the tail current is reduced in the same radial distance range, the magnitude of the B_X component of the lobe magnetic field is reduced (Figure 2b). Thus as the current disruption region expands tailward from the earthward side of the spacecraft, the associated magnetic signature would be first a decrease in B_Z, then a decrease in $|B_X|$, followed by an increase in B_Z. This is exactly the sequence of magnetic perturbations observed by Interball and IMP 8.

[16] For the 24 November 1996 event the expansion velocity is estimated from the spacecraft separation and the delay time to be 460 km/s. It is noteworthy that even at Interball ($X = -26.4\ R_E$) the start of the B_X decrease delayed from the substorm onset by 4 min. If we trace back in time

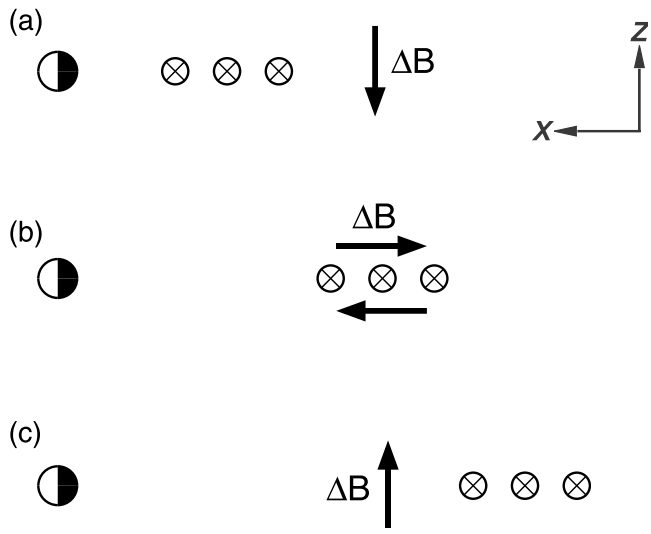

Figure 2. Schematic explanation of the phase relationship between B_X and B_Z in terms of the tailward expansion of the current disruption region. Current disruption is depicted as perturbation currents flowing from dusk to dawn. As the current disruption region expands tailward from the earthward side of the spacecraft, the spacecraft observes (a) a decrease in B_Z, (b) reduction of $|B_X|$, and (c) an increase B_Z. (Modified from Figure 1 of *Ohtani et al.* [1992]).

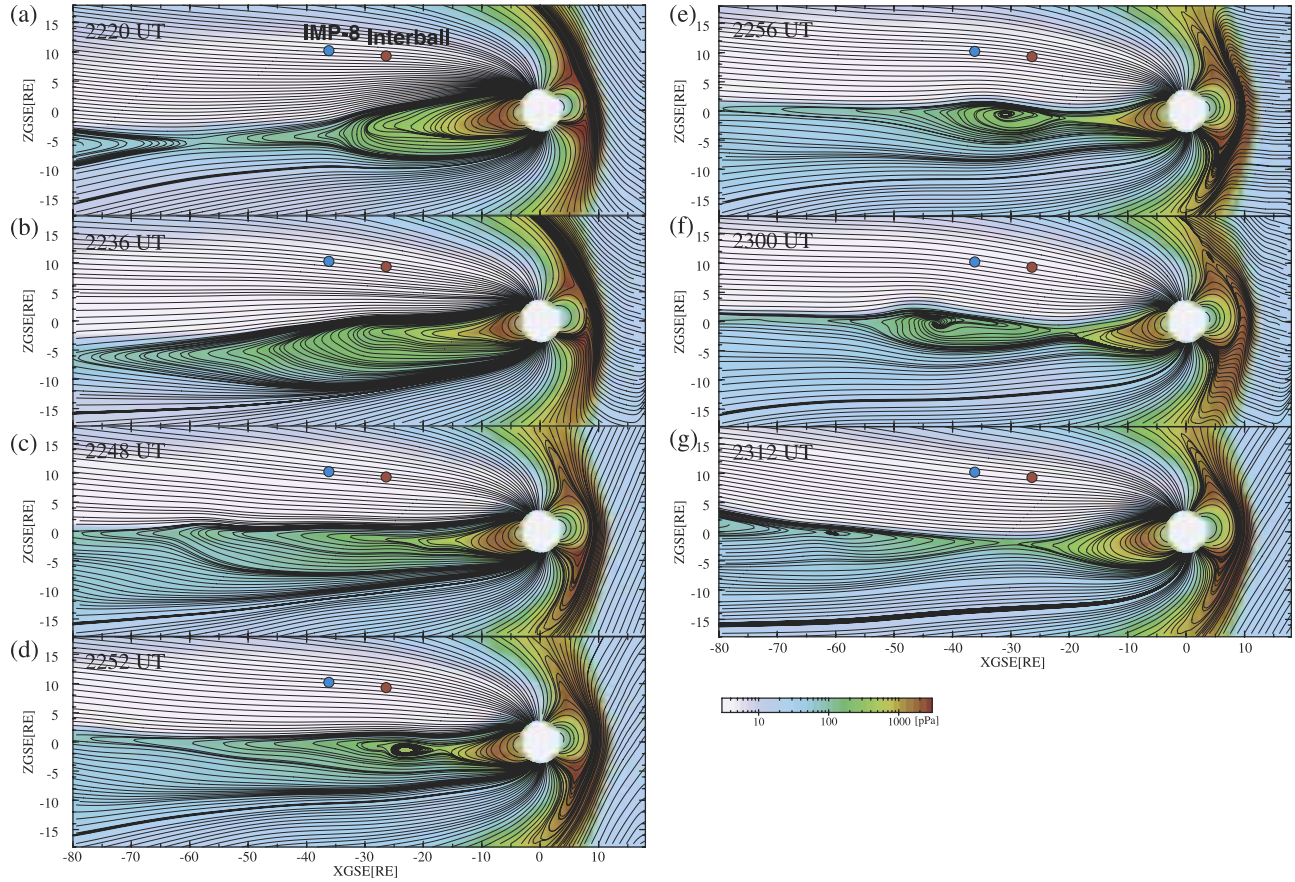

Figure 3. Magnetic field lines (solid lines) and plasma pressure in pPa (colors) of the model magnetosphere at different times.

using the estimated propagation velocity, the X distance of the initial current disruption is estimated to be at $X = -9\ R_E$.

3. Global MHD Simulation

3.1. Overall Sequence of the Modeled Tail Dynamics

[17] In this section we reexamine the overall result of the global MHD simulation [*Raeder et al.*, 2001] from the viewpoint of tail dynamics. Whereas the observations identified the onset of this substorm event at 2227 UT (section 2), the onset of the simulated high-latitude negative bay (Figure 2 of *Raeder et al.* [2001]) occurred about 5 min earlier, which was identified by acceleration of the decrease of simulated X components in the auroral zone. On the other hand, the modeled lobe magnetic field at the Interball and IMP-8 locations started to decrease 7–8 min later than actually observed (section 3.2). Thus there are some differences in timing between the simulation and the observations. Nevertheless, the result of the simulation provides useful new insight about tail substorm dynamics as will be addressed later.

[18] Figure 3 shows tail magnetic configurations (lines) and plasma pressure distributions (color coded) at $Y = 0$ for different epochs; all coordinates are given in the GSE system. The red and blue circles mark the locations of Interball and IMP-8, respectively, projected onto the X-Z plane. Remember that both Interball and IMP-8 were located close to the midnight meridian in the event (section 2).

[19] Figure 3a represents the tail configuration at 2220 UT. An X-line geometry can be found around $X = -58\ R_E$. This neutral line has stayed closer to the Earth before (not shown) and is presumably related to enhanced convection during the growth phase but not to the substorm trigger. The neutral line retreats farther tailward and exits from the left side of the panel by 2236 UT (Figure 3b). Comparison between the 2220 and 2236 UT panels reveals significant stretching of the tail magnetic configuration especially within 25 R_E from the Earth. As will be shown later (Figure 4b), the associated plasma flow is directed tailward outside of 10 R_E and seems to be triggered internally. The flow starts to develop after 2220 UT and therefore may be related to the 2227 UT onset of the intensification of the modeled auroral electrojet. The plasma sheet gets further stretched till 2248 UT (Figure 3c). Note that compared to the configuration at 2236 UT, the stretched magnetic field in the core part of the plasma sheet extends farther down the tail. This plasma-sheet stretching takes place after the modeled substorm onset, which will be addressed later in terms of the changes of the tail current intensity.

[20] At 2252 UT (Figure 3d) a plasmoid (or flux rope) is formed inside the plasma sheet, which is created by the newly formed X-line at $X = -17\ R_E$; the structure will be simply referred to as plasmoid in the rest of the paper. The plasmoid continuously grows as it extends tailward (Figures 3d–3f), and it is about to be released at 2300 UT. By 2312 UT (Figure 3g) the center of the plasmoid (O-line)

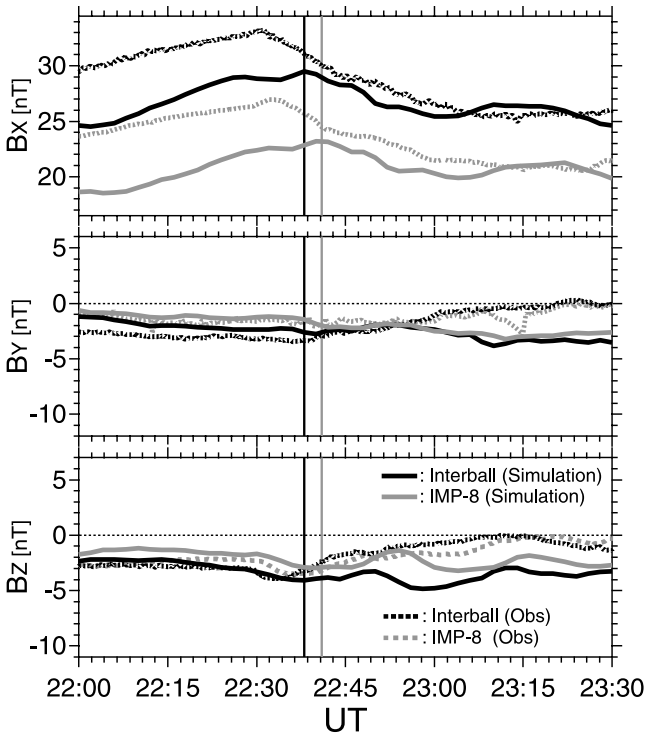

Figure 4. Comparison between the observed and simulated magnetic fields. The Interball (black dashed) and IMP 8 (gray dashed) measurements are compared with the modeled magnetic fields at $X = -26$ (black solid) and -36 (gray solid) R_E.

has exited from the left side of the panel. Note that as the neutral line retreats tailward, which continues even after 2312 UT (not shown), the near-Earth plasma sheet becomes thicker and the magnetic field dipolarizes.

3.2. Modeled Magnetic Signatures at Spacecraft Positions

[21] In Figure 4 we compare the Interball and IMP 8 observations (dotted lines) with magnetic variations at the satellite positions modeled by the global MHD simulation (solid lines). The time resolution of the simulation data is 2 min. There are some similarities as well as differences between the simulation and the observation.

[22] The simulation has reproduced an overall sequence of the observed change of B_X, which first increased and then decreased in association with the storage and release of the lobe magnetic field energy; the vertical lines mark the peaks of simulated B_X at the two satellite positions. However, the sequence of reproduced B_X is more structured, which as will be shown later, can be interpreted in terms of the repeated occurrence of tail current surges. The modeled B_X change also propagates tailward, and the propagation velocity, 350 km/s, is slower than, but in the same range as, the estimate from the observations, 460 km/s. It is also noteworthy that the relative timing of the variations of B_X and B_Z is somewhat similar to the observation. B_Z tends to decrease and increase before and after the maxima of B_X, respectively. There is another dip in B_Z at later time. No noticeable feature can be found for modeled B_Y as is the case for the observation.

[23] It is interesting to address the sequence of the reproduced magnetic perturbations in the context of the global tail dynamics. B_X reaches its maximum at 2238 and 2240 UT at the Interball and IMP-8 locations, respectively, and then as B_X decreases, B_Z slightly increases. Thus the local magnetic field dipolarizes or becomes less stretched. At the same time, however, the overall tail configuration continues to be stretched; compare Figures 3b and 3c. At 2252 UT the Interball satellite is located above the plasmoid (Figure 3d), when the decrease of B_X becomes gradual. This feature may be attributed to the balance of two competing effects, that is, the decrease in B_X associated with the global relaxation of the tail configuration and the local increase in B_X owing to the squeezed lobe magnetic flux by the plasmoid formation. The accompanied decrease in B_Z is consistent with the orientations of lobe magnetic field lines draping the earthward side of the plasmoid, and the final increase in B_Z corresponds to the recovery/thickening of the plasma sheet. The delay between Interball and IMP-8 signature can be attributed to the tailward motion of the plasmoid.

3.3. Simulated Current Systems in the Magnetotail

[24] Figure 5 shows the (1) perpendicular and (2) pressure gradient current densities by colors in the X-UT frame at midnight. Note that both Interball and IMP 8 were located in the midnight sector, and the horizontal axis of Figure 5 covers the same interval as Figure 4. The current densities shown are averages over $[-14, +6]$ R_E in Z. Since this Z range for averaging is fixed and it includes the entire plasma sheet (Figure 3), Figure 5 also tells us how the total intensity, the current integrated in Z over the plasma sheet, of each electric current component changes in time and X.

[25] The tail current is generally more intense closer to the Earth (Figure 5a). The most noticeable feature is the current intensification that takes place early in the interval, which corresponds to the substorm growth phase. At $X > -30$ R_E the current density tends to increase until around 2225 UT and then decrease; this reduction is likely to be related to the intensification of the modeled auroral electrojet. On the other hand, farther down the tail, the current intensification extends continuously. Two similar extensions of tail current intensifications are noticeable: one starting at $X = -15$ R_E around 2232 UT and another at $X = -18$ R_E around 2248 UT. We refer to these features as tail current surges in the following.

[26] Comparison between Figures 5a and 5b reveals that the perpendicular current is mostly driven by the pressure gradient. We found that the contribution of the inertia current to the total perpendicular current (not shown) is less than 5% on average and it rarely exceeds 20% even locally. Thus the tail current dynamics should be explained mostly in terms of the spatial distribution and temporal change of the plasma pressure.

[27] Figure 6a shows the average density of the pressure gradient current by colors in the same way as Figure 5b but with contours of the maximum plasma pressure at $[-14, 6]$ R_E in Z, which should be a good proxy of the plasma pressure at the neutral sheet. The areas of high plasma pressure extend tailward along with tail current surges. Since the plasma-sheet plasma pressure needs to be balanced with the lobe magnetic pressure, the contours of the

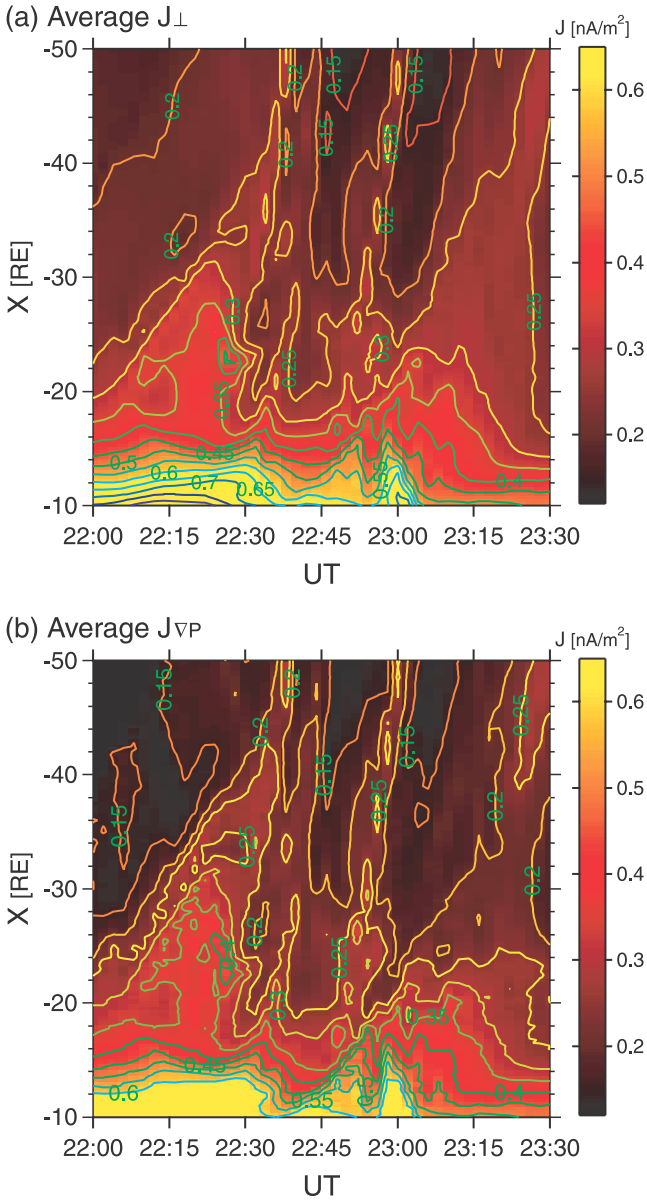

Figure 5. The average densities of (a) the total perpendicular current and (b) the pressure gradient current in the X-UT frame. The current density were calculated by averaging from -6 to $+14$ R_E in Z at $Y = 0$.

maximum plasma pressure can be regarded as those of B_X in the tail lobe. Thus the structured variations of the modeled B_X at the satellite positions (Figure 4) can be attributed to the repeated tailward extensions of high plasma-pressure regions. The contours of the plasma pressure follow those of the pressure gradient current density approximately but not exactly, and the detailed inspection reveals that tail current surges tend to be located a little tailward of the high plasma-pressure regions. This is so because the pressure gradient current is determined by the gradient of the plasma pressure (and the magnetic field strength) but not by the plasma pressure itself.

[28] Figure 6b is the same as Figure 6a but with the contours of the directional (positive and negative for earthward and tailward flows, respectively) maximum X-component flow velocity perpendicular to the magnetic field. Around the beginning of the interval shown (2200 UT), there is no noticeable flow close to the Earth, and the bifurcation of earthward and tailward flows can be found in the midtail region, which moves tailward along with a neutral line (Figure 3a). Closer to the Earth, the area of intense tail current expands tailward. Around 2220 UT a tailward flow starts to develop at $X = -26$ R_E, the area of which expands both earthward and tailward. This tailward plasma motion is related to the stretching of the tail magnetic field (Figure 3) and also to the tailward extension of the high plasma pressure region (Figure 6a). The localization of the initial tailward flow in X suggests that the overall process is triggered internally as an effect of the tail current intensification. The tail current gets weakened at $X >$

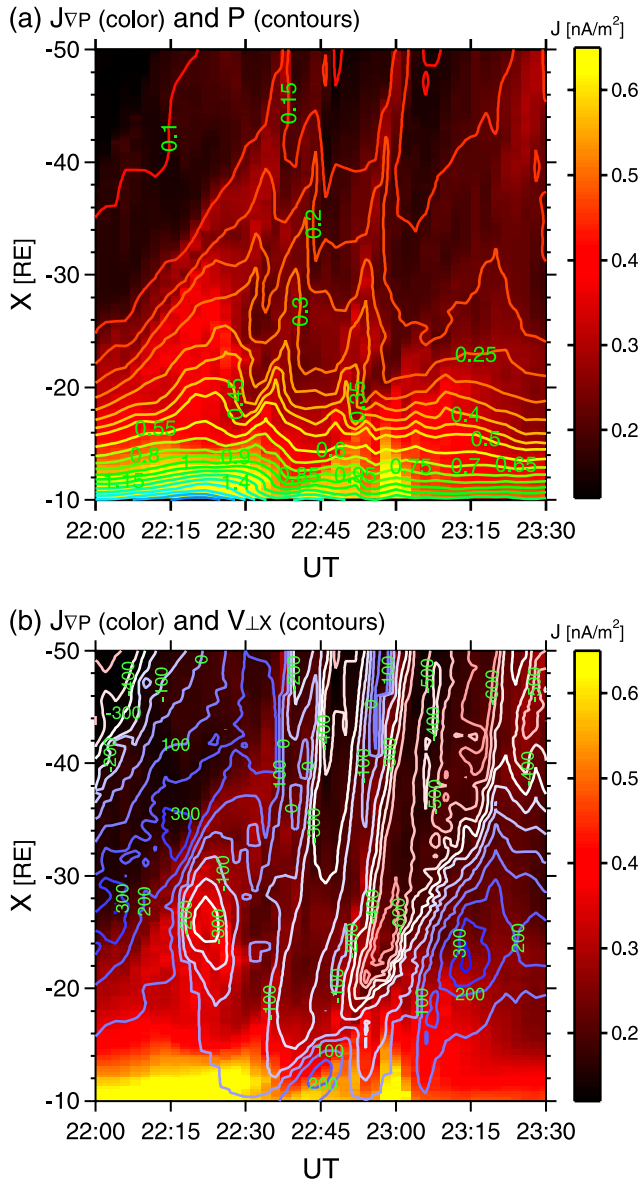

Figure 6. Contours of (a) the maximum plasma pressure in nPa and (b) the maximum X-component perpendicular flow velocity in km/s superposed on the top of the average pressure gradient current density shown by colors.

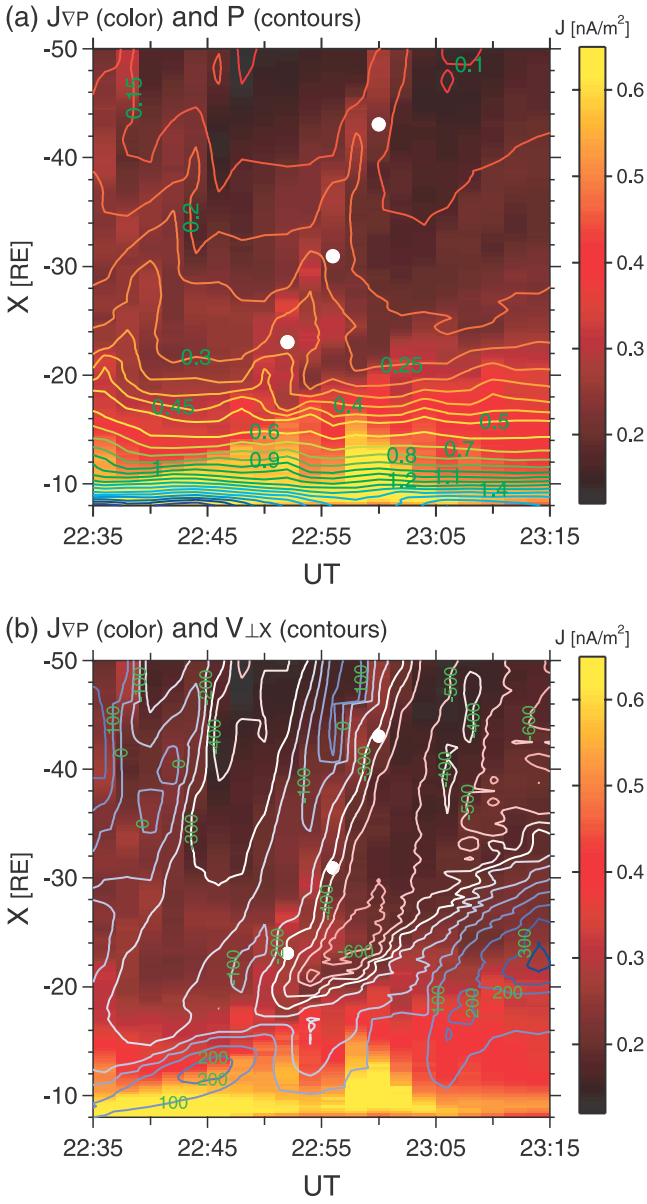

Figure 7. The same as Figure 6 except for 2235–2315 UT. The white dots represent the locations of the *O*-type neutral line at different times determined from Figure 3.

-30 R_E as the tailward flow subsides, whereas farther tailward, it becomes more intense as the plasma pressure enhances. Thus it appears that the tailward flow redistributes the tail current more widely in X, which also explains why the modeled B_X components at Interball and IMP-8 tend to increase even after the intensification of the modeled auroral electrojet. The second tail current surge, which starts at $X = -15$ R_E around 2232 UT, is also accompanied by the transient tailward extension of a high plasma pressure region and also by a tailward plasma flow.

[29] Later, in the near-Earth region ($X > -15$ R_E), an earthward flow develops, and most interestingly, when it subsides, a fast tailward flow is formed just on its tailward side. Figure 7b shows a close-up view of this feature in the same format as Figure 6b with an X range starting closer to the Earth. The formation of the earthward flow starts in the bottom left corner of the panel. Plasma is flowing tailward just on its tailward side, which corresponds to the further stretching of the near-Earth magnetic field (Figure 3). As the area of the earthward flow moves tailward, the flow velocity increases and reaches its peak, ~250 km/s, at $X = -12$ R_E at 2245 UT. The new tailward flow starts to develop at 2250 UT around $X = -16$ R_E. This tailward flow is associated with the formation of a near-Earth neutral line (Figure 3d). The white dots in Figure 7 mark the locations of the *O*-type neutral line at different times (Figures 3d–3f). The *O*-line moves tailward along with the background plasma, although the plasmoid has not been detached yet (Figure 3).

[30] This tailward flow is accompanied by the intensification of the pressure gradient current (tail current surge), which stays ahead of the flow. As shown in Figure 7a, the contours of the plasma pressure follow the motion of the O-line, and the pressure gradient, which drives the current, increases ahead of the O-line. Although this tail current surge appears to be similar to the previous ones (Figure 6), its generation mechanism is different. Whereas the previous ones are accompanied by the stretching of the tail magnetic field, this last one is caused by the ejection of the plasmoid.

4. Discussion and Summary

[31] In the substorm event of 24 November 1996, the Interball and IMP-8 satellites were located at $X = -26$ and -36 R_E, respectively, in the northern tail lobe and observed the B_X component to increase and decrease. The decrease in B_X was accompanied by the subsequent occurrence of a decrease and an increase in B_Z with the phase relationship that the previous studies [*Jacquey et al.*, 1991; *Ohtani et al.*, 1992] interpreted in terms of the tailward expansion of the current disruption region. The time lag between the Interball and IMP-8 signatures also indicates the tailward propagation of the signature. A global MHD simulation was conducted for this event [*Raeder et al.*, 2001], which provides an ideal opportunity to consider the observation in terms of global substorm dynamics.

[32] We have found both similarities and differences between the observations and the modeled magnetic variations at the satellite positions. The simulation reproduced an increase and a decrease in the lobe magnetic field strength, corresponding to the storage and release of the lobe magnetic energy in the course of the substorm. Note also that in both simulation and observation, this energy storage and release take place after the substorm onset. Whereas the simulated signature is more structured, it shows the phase relationship between B_X and B_Z similar to what was observed by the satellites. Moreover, the simulated magnetic variations also propagate tailward at a velocity (350 km/s) similar to the velocity estimated from the observation (460 km/s).

[33] The result of the simulation shows that the tail current is driven mostly by the plasma pressure gradient and the contribution of the inertia current is minimal, suggesting that the plasma pressure plays the main role in the tail electrodynamics. The dominant role of the plasma pressure was also reported by *Birn et al.* [1999] based on an MHD simulation in the context of the tail current reduction caused by the fast plasma flow.

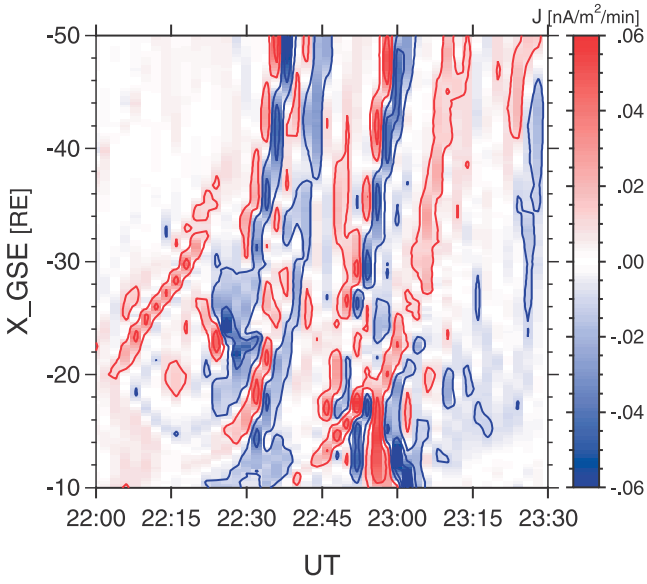

Figure 8. The change of the average perpendicular current density.

[34] The most noticeable feature of the simulated tail dynamics is the repeated occurrence of tail current surges, that is, the intensifications of the tail current that propagate tailward. In association with each tail current surge, the region of high plasma pressure propagates tailward. At its propagation front, the pressure gradient increases, which drives an intensified tail current. The timescale (~5 min) of the associated intensification is much shorter than the typical duration of the substorm growth phase. Instead, those tail current surges, including the very initial one, may be regarded as an expansion (or onset) phase feature because they start in the near-Earth region.

[35] We found that there is more than one cause for tail current surges. The very first surge is associated with the stretching of the tail magnetic field. The associated tailward plasma flow redistributes the plasma pressure in such a way that the temporal intensification of the tail current propagates tailward along with the high plasma pressure region. On the other hand, the last tail current surge is related to the initiation of near-Earth reconnection and the formation of a plasmoid. On the tailward side of an *O*-type neutral line but inside the plasmoid, the pressure gradient current is intensified, which propagates tailward in association with the release of the plasmoid.

[36] An interesting question is what we can learn from the simulation for this event; this question may be a challenge since the simulation shows tail current surges as a predominant feature, whereas the magnetic signature observed by Interball and IMP-8 has been regarded as a manifestation of the release of the lobe magnetic energy.

[37] *Ohtani et al.* [1992] have proposed two different ways to explain the phase relationship between the observed B_X and B_Z variations. One explanation, which has already been described in section 2 (Figure 2), is based on the tailward expansion of the current disruption region. To examine the temporal change of the modeled tail current, we differentiated the average perpendicular current density (Figure 5a). Figure 8 shows the result. For the earlier half of the interval, two blue (current reduction) stripes are noticeable, which propagate tailward. Since each tail current surge consists of tail current intensification and subsequent current reduction (Figure 5a), it is expected that the current reduction propagates tailward following the intensification. However, Figure 8 reveals that in contrast to the current intensification, which is rather fragmented, the current disruption propagates systematically tailward, which favors the idea depicted in Figure 2. The reason for that is not self-evident; the magnetotail may adjust its configuration more easily to reach a lower-energy status through tail current disruption. The present result suggests that although the change of the tail current intensity may be simplified as the tailward expansion of the current disruption region, the overall dynamics of the tail current could be far more complex than depicted in Figure 2.

[38] Figure 9 schematically shows the other explanation, which assumes that a neutral line passes by the spacecraft from its earthward side. The figure depicts it as an equivalent earthward motion of the spacecraft relative to the neutral line. First, the spacecraft starts to observe a southward deflection of the magnetic field, and $|B_X|$ tends to decrease as the neutral line approaches the spacecraft. Once the neutral line passes the radial distance of the satellite, B_Z starts to increase. Thus the time sequence of B_X and B_Z variations is just the same as expected from the tailward expansion of the current disruption region. Figure 3 shows that the modeled neutral line is indeed formed on the earthward side of Interball and IMP-8 and that it moves tailward passing by the radial distances of these satellites; the neutral line moves tailward continuously after 2312 UT (Figure 3g). Although the modeled magnetic variations at the satellite positions are consistent with the idea shown in Figure 9 (see Figure 4 for the interval of 2250–2315 UT), they are not as systematic as were actually observed in this event (Figure 1). This may be attributed to structured variations of the tail current intensity (Figure 8).

[39] The simulation shows that the tailward passage of a plasmoid is also accompanied by an intensification of the tail current followed by an immediate reduction (Figures 7 and 8). The preceding intensification takes place on the tailward side of an *O*-line. On the earthward side, the tail current is reduced in its intensity, and this current reduction propagates tailward as the plasmoid expands/moves tail-

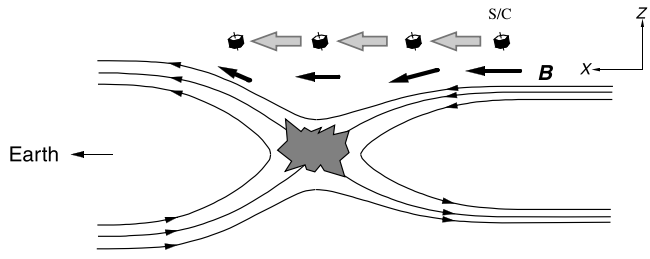

Figure 9. Schematic explanation of the phase relationship between B_X and B_Z in terms of the tailward motion of a neutral line, which is depicted equivalently as the earthward motion of the spacecraft. As a neutral line moves tailward (the spacecraft moves earthward as depicted), the spacecraft observes a decrease in B_Z, reduction of $|B_X|$, and an increase in B_Z. (Adopted from Figure 7 of *Ohtani et al.* [1992]).

ward. We therefore infer that the tailward movement of a neutral line causes a magnetic signature very similar to what is caused by a tail current surge without a neutral line. Furthermore, in terms of the associated change of the tail current intensity and the propagation speed, there is no quantitative difference in our model between tail current surges with and without the neutral line formation. Thus it may be extremely difficult, if not impossible, to distinguish based on the lobe magnetic field measurement whether or not the observed signature is related to the reconnection. The most straightforward and possibly the only way to make such a distinction might be to simultaneously measure the magnetic field in the plasma sheet at the same (X, Y) coordinates as the lobe measurement.

[40] Finally, it is interesting to address the result of the present simulation in terms of substorm trigger models, that is, the pile-up/braking model and the rarefaction wave model (section 1). At first glance, the result of the present simulation appears to be consistent with the rarefaction wave model since the magnetic field stretching propagates tailward from the inner magnetosphere. However, the associated tail current surge is accompanied by an increase, rather than a decrease, of plasma pressure, which is just the opposite of what is expected from the rarefaction wave. However, the last current surge, which is driven by the reconnection, appears to be related to the preceding development of the earthward flow closer to the Earth ($X > -15\ R_E$). The sequence is consistent with the rarefaction model, although more detailed analysis is required for identifying the responsible process in the near-Earth region; one interesting fact is that this near-Earth process is related to the intensification rather than the disruption of the tail current (Figure 7b). It is also difficult to follow the pile-up/braking model in the present simulation. The most critical feature against the model is that the near-Earth neutral line appears to form as a result of a process closer to the Earth, and this near-Earth process itself is not preceded by any fast earthward flow. However, generally speaking, it is essential for identifying the trigger mechanism to understand the X-Y structure of the associated plasma dynamics, which is beyond the scope of the present study.

[41] Tail substorm dynamics have been a major issue of magnetospheric physics since the beginning of the satellite observation. The limited spatial coverage of in situ measurements is often blamed for the lack of definitive interpretations of satellite observations, which, however, is likely to be overcome to some extent, if not completely, by future multisatellite missions. Meanwhile global MHD simulations motivate us to explore aspects and ideas that would draw very little attention if only in situ observations were available. Most people would interpret the increase in B_X and the following decrease observed in the 24 November 1996 event as features associated with the local growth and expansion phases, respectively. On the other hand, the intensification and reduction of the tail current modeled by the present simulation is an effect of a near-Earth process propagating tailward, whether they are related to the stretching of the tail configuration or to the tailward motion of the neutral line. Despite the fact that we will never know how precisely the present simulation actually modeled the 24 November 1996 event, it would be interesting to ask ourselves if (or how far) we could consider such an alternative explanation without the present simulation. We believe that the present study not only sheds new light about tail substorm dynamics but also provides a good exercise for evaluating the potential of the modeling effort for substorm study in general.

[42] **Acknowledgments.** We are grateful to S. Romanov and D. G. Sibeck for the Interball magnetic field data and R. P. Lepping for the IMP-8 magnetometer data. Work at APL was supported by grants NAG5-12050 from the National Aeronautics and Space Administration and ATM-9901282 from the National Science Foundation. Work at UCLA was supported by grants ATM 00-84483 and ATM 01-12555 from the National Science Foundation. Computations were performed at the San Diego Supercomputer Center and the National Center for Supercomputer Applications.

[43] Lou-Chuang Lee thanks Michael Wiltberger and another reviewer for their assistance in evaluating this paper.

References

Akasofu, S.-I. (1964), The development of the auroral substorm, *Planet. Space Sci.*, *12*, 273.

Akasofu, S.-I. (1972), Magnetospheric substorms: A model, in *Solar Terrestrial Physics*, part 3, pp. 131–151, edited by M. Dyer, D. Reidel, Norwell, Mass.

Baker, D. N., T. I. Pulkkinen, V. Angelopoulos, W. Baumjohann, and R. L. McPherron (1996), Neutral line model of substorms: Past results and present view, *J. Geophys. Res.*, *101*, 12,975.

Birn, J., M. Hesse, G. Haerendel, W. Baumjohann, and K. Shiokawa (1999), Flow braking and the substorm current wedge, *J. Geophys. Res.*, *104*, 19,895.

Chao, J. K., J. R. Kan, A. T. Y. Lui, and S.-I. Akasofu (1977), A model for thinning of the plasma sheet, *Planet. Space Sci.*, *25*, 703.

Cheng, C. Z., and A. T. Y. Lui (1998), Kinetic ballooning instability for substorm onset and current disruption observed by AMPTE/CCE, *Geophys. Res. Lett.*, *25*, 4091.

Cummings, W. D., J. N. Barfield, and P. J. Coleman Jr. (1968), Magnetospheric substorms observed at the synchronous orbit, *J. Geophys. Res.*, *73*, 6887.

Erickson, G. M., N. C. Maynard, W. J. Burke, G. R. Wilson, and M. A. Heinemann (2000), Electromagnetics of substorm onsets in the near-geosynchronous plasma sheet, *J. Geophys. Res.*, *105*, 25,265.

Friedrich, E., J. C. Samson, I. Voronkov, and G. Rostoker (2001), Dynamics of the substorm expansive phase, *J. Geophys. Res.*, *106*, 13,145.

Hesse, M., and J. Birn (1991), On dipolarization and its relation to the substorm current wedge, *J. Geophys. Res.*, *96*, 19,417.

Jacquey, C., J.-A. Sauvaud, and J. Dandouras (1991), Location and propagation of the magnetotail current disruption during substorm expansion: Analysis and simulation of an ISEE multi-onset event, *Geophys. Res. Lett.*, *18*, 389.

Jacquey, C., J.-A. Sauvaud, J. Dandouras, and A. Korth (1993), Tailward propagating cross-tail current disruption and dynamics of near-Earth tail: Multi-point measurement analysis, *Geophys. Res. Lett.*, *20*, 983.

Lopez, R. E., and A. T. Y. Lui (1990), A multisatellite case study of the expansion of a substorm current wedge in the near-Earth magnetotail, *J. Geophys. Res.*, *95*, 8009.

Lui, A. T. Y. (1991), Extended consideration of a synthesis model for magnetospheric substorms, in *Magnetospheric Substorms*, *Geophys. Monogr. Ser.*, vol. 64, edited by J. R. Kan et al., p. 43, AGU, Washington, D.C.

Lui, A. T. Y. (1996), Current disruption in the Earth's magnetosphere: Observations and models, *J. Geophys. Res.*, *101*, 13,067.

Lui, A. T. Y., C.-I. Chang, A. Mankofsky, H. K. Wong, and D. Winske (1991), A cross-field current instability for substorm expansions, *J. Geophys. Res.*, *96*, 11,389.

Lyons, L. R., R. L. McPherron, E. Zesta, G. D. Reeves, J. B. Sigwarth, and L. A. Frank (2001), Timing of substorm signatures during the November 24, 1996, Geospace Environment Modeling event, *J. Geophys. Res.*, *106*, 349.

McPherron, R. L., C. T. Russell, and M. P. Aubry (1973), Satellite studies of magnetospheric substorms on August 15, 1968: 9. Phenomenological model for substorms, *J. Geophys. Res.*, *78*, 3131.

Nagai, T., M. Fujimoto, Y. Saito, S. Machida, T. Terasawa, R. Nakamura, T. Yamamoto, T. Mukai, A. Nishida, and S. Kokubun (1998), Structure and dynamics of magnetic reconnection for substorm onsets with Geotail observations, *J. Geophys. Res.*, *103*, 4419.

Ohtani, S., S. Kokubun, R. C. Elphic, and C. T. Russell (1988), Field-aligned current signatures in the near-tail region: 1. ISEE observations in the plasma sheet boundary layer, *J. Geophys. Res.*, *93*, 9709.

Ohtani, S., S. Kokubun, and C. T. Russell (1992), Radial expansion of the tail current disruption during substorms: A new approach to the substorm onset region, *J. Geophys. Res.*, *97*, 3129.

Ohtani, S., F. Creutzberg, T. Mukai, H. Singer, A. T. Y. Lui, M. Nakamura, P. Prikryl, K. Yumoto, and G. Rostoker (1999), Substorm onset timing: The December 31, 1995, event, *J. Geophys. Res.*, *104*, 22,713.

Petrukovich, A. A., T. Mukai, S. Kokubun, S. Romanov, Y. Saito, T. Yamamoto, and L. M. Zelenyi (1999), Substorm-associated pressure variations in the magnetotail plasma sheet and lobe, *J. Geophys. Res.*, *104*, 4501.

Raeder, J., and N. C. Maynard (2001), Foreward, *J. Geophys. Res*, *106*, 345.

Raeder, J., R. L. McPherron, L. A. Frank, S. Kokubun, G. Lu, T. Mukai, W. R. Paterson, J. B. Sigwarth, H. Singer, and J. A. Slavin (2001), Global simulation of the Geospace Environment Modeling substorm challenge event, *J. Geophys. Res.*, *106*, 381.

Roux, A., S. Perraut, P. Robert, A. Morane, A. Pedersen, A. Korth, G. Kremser, B. Aparicio, D. Rodgers, and R. Pellinen (1991), Plasma sheet instability related to the westward traveling surge, *J. Geophys. Res.*, *96*, 17,697.

Samson, J. C., L. R. Lyons, B. Xu, F. Creutzberg, and P. T. Newell (1992), Proton aurora and substorm intensifications, *Geophys. Res. Lett.*, *19*, 2167.

Shiokawa, K., W. Baumjohann, G. Haerendel, G. Paschmann, J. G. Fennell, E. Friis-Christensen, H. Lühr, G. D. Reeves, C. T. Russell, P. R. Sutcliffe, and K. Takahashi (1998), High-speed ion flow, substorm current wedge, and multiple Pi 2 pulsations, *J. Geophys. Res.*, *103*, 4491.

Slinker, S. P., J. A. Fedder, J. M. Ruohoniemi, and J. G. Lyon (1996), Global MHD simulation of the magnetosphere for November 24, 1996, *J. Geophys. Res*, *106*, 361.

Yoon, P. H., and A. T. Y. Lui (2001), On the drift-sausage mode in one-dimensional current sheet, *J. Geophys. Res.*, *106*, 1939.

Yoon, P. H., A. T. Y. Lui, and H. K. Wong (1998), Two-fluid theory of drift-kink instability in one-dimensional neutral sheet, *J. Geophys. Res.*, *103*, 11,875.

S. Ohtani, Applied Physics Laboratory, Johns Hopkins University, 11000 Johns Hopkins Road, Laurel, MD 20723-6099, USA. (ohtani@jhuapl.edu)

J. Raeder, Space Science Center, University of New Hampshire, 39 College Road, Durham, NH 03824, USA. (j.raeder@unh.edu)